



TGF β -Associated Signature Predicts Prognosis and Tumor Microenvironment Infiltration Characterization in Gastric Carcinoma

Siyuan Liu^{1†}, Zhenghao Li^{1†}, Huihuang Li², Xueyi Wen¹, Yu Wang¹, Qilin Chen¹ and Xundi Xu^{1,3*}

¹Hunan Provincial Key Laboratory of Hepatobiliary Disease Research and Division of Hepato-Biliary-Pancreatic Surgery, Department of General Surgery, The Second Xiangya Hospital, Central South University, Changsha, China, ²Department of Urology Surgery, Xiangya Hospital, Central South University, Changsha, China, ³Department of General Surgery, The South China Hospital, Shenzhen University, Shenzhen, China

OPEN ACCESS

Edited by:

Yichuan Liu,
Children's Hospital of Philadelphia
(CHOP), United States

Reviewed by:

Xuming Zhu,
Icahn School of Medicine at Mount
Sinai, United States
Xiaohan Ren,
Nanjing Medical University, China

*Correspondence:

Xundi Xu
xuxundi@csu.edu.cn

[†]These authors have contributed
equally to this work and share first
authorship

Specialty section:

This article was submitted to
Computational Genomics,
a section of the journal
Frontiers in Genetics

Received: 19 November 2021

Accepted: 19 April 2022

Published: 18 May 2022

Citation:

Liu S, Li Z, Li H, Wen X, Wang Y,
Chen Q and Xu X (2022) TGF β -
Associated Signature Predicts
Prognosis and Tumor
Microenvironment Infiltration
Characterization in Gastric Carcinoma.
Front. Genet. 13:818378.
doi: 10.3389/fgene.2022.818378

Background: Gastric carcinoma (GC) is a carcinoma with a high incidence rate, and it is a deadly carcinoma globally. An effective tool, that is, able to predict different survival outcomes for GC patients receiving individualized treatments is deeply needed.

Methods: In total, data from 975 GC patients were collected from TCGA-STAD, GSE15459, and GSE84437. Then, we performed a comprehensive unsupervised clustering analysis based on 54 TGF β -pathway-related genes and correlated these patterns with tumor microenvironment (TME) cell-infiltrating characteristics. WGCNA was then applied to find the module that had the closest relation with these patterns. The least absolute shrinkage and selection operator (LASSO) algorithm was combined with cross validation to narrow down variables and random survival forest (RSF) was used to create a risk score.

Results: We identified two different TGF β regulation patterns and named them as TGF β Cluster 1 and Cluster 2. TGF β Cluster 1 was linked to significantly poorer survival outcomes and represented an inflamed TME subtype of GC. Using WGCNA, a module (magenta) with the closest association with the TGF β clusters was identified. After narrowing down the gene list by univariate Cox regression analysis, the LASSO algorithm and cross validation, four of the 243 genes in the magenta module were applied to build a risk score. The group with a higher risk score exhibited a considerably poorer survival outcome with high predictive accuracy. The risk score remained an independent risk factor in multivariate Cox analysis. Moreover, we validated this risk score using GSE15459 and GSE84437. Furthermore, we found that the group with a higher risk score represented an inflamed TME according to the evidence that the risk score was remarkably correlated with several

Abbreviations: TGF, transforming growth factor; GC, gastric carcinoma; STAD, stomach adenocarcinoma; ICI, immune checkpoint inhibitor; PD-1 and PD-L1, programmed cell death-1 and its ligand; MSI, microsatellite instability; TME, tumor microenvironment; RNA-seq, RNA sequencing; FPKM, fragments per kilobase per million mapped fragments; TPM, transcripts per kilobase million; GEO, Gene Expression Omnibus; ssGSEA, single-sample gene-set enrichment analysis; LASSO, least absolute shrinkage and selector operation; ROC, receiver-operating characteristic; Th1, T helper 1; NK, natural killer; DC, dendritic cell; ECM, extracellular matrix; GEP, gene expression profiles; BMP, bone morphogenetic protein; m6A, RNA modification of N6-methyladenosine; PCA, principal component analysis; AUC, area under the curve.

steps of cancer immunity cycles and a majority of the infiltrating immune cells. Consistently, the risk score was significantly related to immune checkpoint genes and T cell-inflamed gene expression profiles (GEPs), indicating the value of predicting immunotherapy.

Conclusions: We have developed and validated a TGF β -associated signature, that is, capable of predicting the survival outcome as well as depicting the TME immune characteristics of GC. In summary, this signature may contribute to precision medicine for GC.

Keywords: TGF β , prognosis, tumor microenvironment, gastric carcinoma, immunotherapy

INTRODUCTION

Gastric carcinoma (GC) has the fifth highest incidence rate of cancer and the third highest fatality rate globally, causing approximately 723,000 deaths in 2012 (Smyth et al., 2020). Although classic therapies such as chemotherapy and even biological agents are utilized, patients with advanced gastric carcinoma still face an unsatisfactory prognosis. Immune checkpoint inhibitors (ICIs) especially programmed cell death-1 (PD-1) together with its ligand (PD-L1 or B7-H1), have been shown to be essential for the progression of several solid cancers and are likely to become a promising therapeutic target in gastric carcinoma treatment (Coutzac et al., 2019). Several clinical tests evaluating anti-PD-1/PD-L1-based curative methods as both first and later-line treatments have already produced inspiring results (Kang et al., 2017; Fuchs et al., 2018; Janjigian et al., 2018). However, not all patients in this cohort responded to ICI treatment. The primary predictors for immunotherapy effectiveness are likely to be PD-L1 expression together with defects in mismatch repair genes resulting in a microsatellite instability (MSI-H) phenotype (Vrána et al., 2018). All these biomarkers have failed for widespread clinical application because of unsatisfactory predictive accuracy or complex detection methods (Crispen and Kusmartsev, 2020; Hu et al., 2021). There is an urgent need to find robust biomarkers that could provide clues regarding the prognosis and immunotherapy response in GC.

The tumor microenvironment (TME) includes various cell types (fibroblasts, endothelial cells, immune cells, etc.) together with extracellular elements (growth factors, cytokines, extracellular matrix, hormones, etc.) that surround tumor cells and are nourished by a microvascular network (Wu and Dai, 2017). The TME can be generally divided into cold (non-T cell inflamed) and hot (T cell inflamed) conditions, which are mainly based on the production levels of proinflammatory cytokines and the infiltration degree of T cells (Gajewski, 2015). Hot tumors are characterized by T cell infiltration together with immune activated molecular signatures, whereas cold tumors are characterized by T cell exclusion or absence. Generally, more patients in the hot tumor subgroup will respond to immunotherapy, such as ICI therapy (Liu et al., 2020a). Transforming growth factor β (TGF β) is a crucial enforcer of immune homeostasis and tolerance and plays an essential role in the formation of the immune suppression TME (Batlle and Massagué, 2019). In melanoma, the TGF β pathway was reported to play an important role in the formation of ICI resistance (Hugo et al.,

2016). In metastatic urothelial cancer, TGF β signaling was associated with lower response rates to anti-PD-L1 (atezolizumab) therapy (Mariathasan et al., 2018). In GC, TGF β was shown to increase the migration, adhesion and invasion of some GC cell lines but not all (Veen et al., 2021). Therefore, it is necessary to distinguish which patients could respond to therapy. There is no study correlating the TGF β -associated signature with the TME in GC. In this study, we developed a TGF β regulation patterns and risk scores that could predict individual patient survival outcomes and TME characteristics.

MATERIALS AND METHODS

Data Retrieval and Preprocessing

We downloaded the RNA sequencing (RNA-seq) and survival data of TCGA-STAD (stomach adenocarcinoma) from the data portal of UCSC Xena (<https://xenabrowser.net/>) (Goldman et al., 2020). Then, we transformed the fragments per kilobase per million mapped fragments (FPKM) value into transcripts per kilobase million (TPM) value. We included 350 GC patients for further analysis after moving duplicates and patients without clinical information. For Gene Expression Omnibus (GEO) databases, we downloaded the expression matrices and platforms of the GSE15459 (GPL570) and GSE84437 (GPL6947) using the “GEOquery” R package. The clinical information originating from the databases that we included is summarized in **Supplementary Table S1**.

Consensus Clustering

We systematically identified 54 TGF β -pathway-related genes from the Molecular Signatures Database (MSigDB) (**Supplementary Table S2**). We then performed unsupervised clustering analysis to comprehensively identify two distinct TGF β related patterns using the k-means method implemented in the “ConsensusClusterPlus” R package. We conducted 1,000 repetitions to guarantee the stability of our classification (Wilkerson and Hayes, 2010).

Gene Set Variation Analysis

“Limma” R package was used to filtered out the differentially expressed genes (DEGs) between different TGF β regulation patterns and then the genes were ordered by fold change (FC). The gene sets of “c5.all.v7.1.symbolsGO” and “c2.cp.kegg.v7.1.symbolsKEGG” were downloaded from MSigDB database for running GSEA analysis. Adjusted *p* with value less than 0.05 was considered as statistically significance.

Tumor Microenvironment Cell Infiltration

The activated levels of the anticancer immune response were all downloaded from <http://biocc.hrbmu.edu.cn/TIP/> using the TPM value of TCGA-STAD (Chen and Mellman, 2013; Xu et al., 2018). Then, we quantified the levels of tumor-infiltrating immune cells (TIICs) using the single-sample gene-set enrichment analysis (ssGSEA) algorithm. The gene sets for calculating specific immune cells were collected from the study reported by Charoentong et al. (2017) (**Supplementary Table S3**) (Charoentong et al., 2017).

Coexpression Module Networks

We conducted a network of gene coexpression to identify the TGF β cluster-related module using the “WGCNA” R package (Langfelder and Horvath, 2008). First, we filtered out bad genes and samples using TPM data from TCGA-STAD. Then, we calculated the connection strength and developed a scale-free network using the filtered data. We examined the scale independence and modules’ average connectivity degree using the gradient method and chose the most suitable power value when setting the degree of independence as 0.85 (Chen et al., 2017). Next, using the selected power value, we generated scale-free gene coexpression networks. We regarded TGF β clusters as a clinical factor and showed the relationship between different modules and clinical factors using heatmap. Finally, we selected the module with the closest relationship with TGF β clusters for further analysis (Li et al., 2021).

Creation and Validation of the Risk Score

First, we performed univariate Cox analysis on genes of the module with the closest relationship with the TGF β clusters to screen genes having prognostic value. Then, the least absolute shrinkage and selector operation (LASSO) algorithm was used for the screened genes. Finally, using the `rfsrc` function in the “randomForestSRC” R package, a TGF β -associated risk score was constructed based on the genes filtered by the LASSO algorithm. Using the median value of the risk score, GC patients were divided into high- and low-risk score groups. We developed a Kaplan-Meier survival curve, and the prognostic significance of the risk score was compared using the log-rank test. The sensitivity and specificity of the risk score for predicting survival outcome were tested by receiver operating characteristic curve (ROC) analysis using the `tROC` R package. The role of predicting the survival outcome of the risk score was further validated in the GSE15459 and GSE84437 databases. Univariate Cox analysis was applied to filter prognostic factors including age, sex, tumor grade, tumor stage, and risk score, and multivariate Cox analysis was further applied to filter independent prognostic factors. Moreover, a systematic nomogram was constructed based on those factors with independent prognostic values in multivariate Cox analysis.

Statistical Analysis

Correlation coefficients between variables were computed using Pearson or Spearman correlation analyses. A *t* test or Mann-Whitney *U* test was applied to calculate the differences in continuous variables. We applied the LASSO algorithm to filter the optimal TGF β associated genes with the best discriminative capability. Then a Kaplan-Meier survival curve was constructed and the prognostic significance of the risk score was compared

using the log-rank test. The sensitivity and specificity of the risk score for predicting survival outcome were tested by ROC-curve analysis using the `tROC` R package. All statistical analyses were conducted with R software (version 4.0.3), and two-sided $p < 0.05$ was set as the significance criterion.

RESULTS

Depicting Transforming Growth Factor β Clusters and Correlating Them With Tumor Microenvironment Infiltration

As shown in **Figure 1A**, most of the 54 TGF β -pathway-related genes were prognostic factors and correlated closely with each other. We demonstrate the comprehensive landscape of gene interactions, connections, and prognostic values. Inspired by these results, we performed a comprehensive unsupervised clustering analysis based on these 54 TGF β -pathway-related genes and two different TGF β regulation patterns named TGF β Cluster 1 and Cluster 2 were identified (**Figure 1B, Supplementary Figures S1A–E**). A total of 182 patients divided into TGF β Cluster 1 exhibited significantly poorer survival outcomes than the other 168 patients divided into Cluster 2 ($p = 0.032$, **Figure 1C**).

Considering the vital role of TGF β in shaping the immune suppression TME, we comprehensively correlated the clusters with immune phenotypes (Batlle and Massagué, 2019). The anticancer immune cycles include the following seven steps: tumor antigen release and presentation (steps 1 and 2), immune system priming and activation (step 3), transferring and invasion of immune cells to tumors (steps 4 and 5), and effector immune cells recognizing and killing cancer cells (steps 6 and 7) (Chen and Mellman, 2013). First, the relationship between TGF β clusters and activities of anticancer immunity cycles enters our field of vision. The activities of cancer cell antigen release, T cell, CD8 T cell, T helper 1 (Th1) cell and monocyte recruitment, and infiltration of immune cells into tumors were significantly higher in TGF β Cluster 1 than Cluster 2. These results indicate that TGF β Cluster 1 might represent an inflamed TME subtype of GC, while TGF β Cluster 2 represents a non-inflamed subtype (**Figure 1D**). Furthermore, we directly calculated the infiltration of immune cells into the TME by the ssGSEA algorithm. Consistent with the anticancer immune response, the majority of immune cells, including activated dendritic cells (DCs), effector memory CD4 T cells, effector memory CD8 T cells, macrophages, natural killer (NK) cells, had significantly higher numbers in TGF β Cluster 1 than in Cluster 2 (**Figure 1E**). In addition, we found that all angiogenesis related pathways were significantly enriched in TGF β Cluster 1, indicating a more active tumor angiogenesis in Cluster 1 (**Supplementary Figure S1F, Supplementary Table S4**).

Key Modules and Hub Genes Related to Transforming Growth Factor β Clusters Identified by WGCNA

We developed TGF β based patterns that could predict survival outcomes and TME infiltration in the previous step. To predict

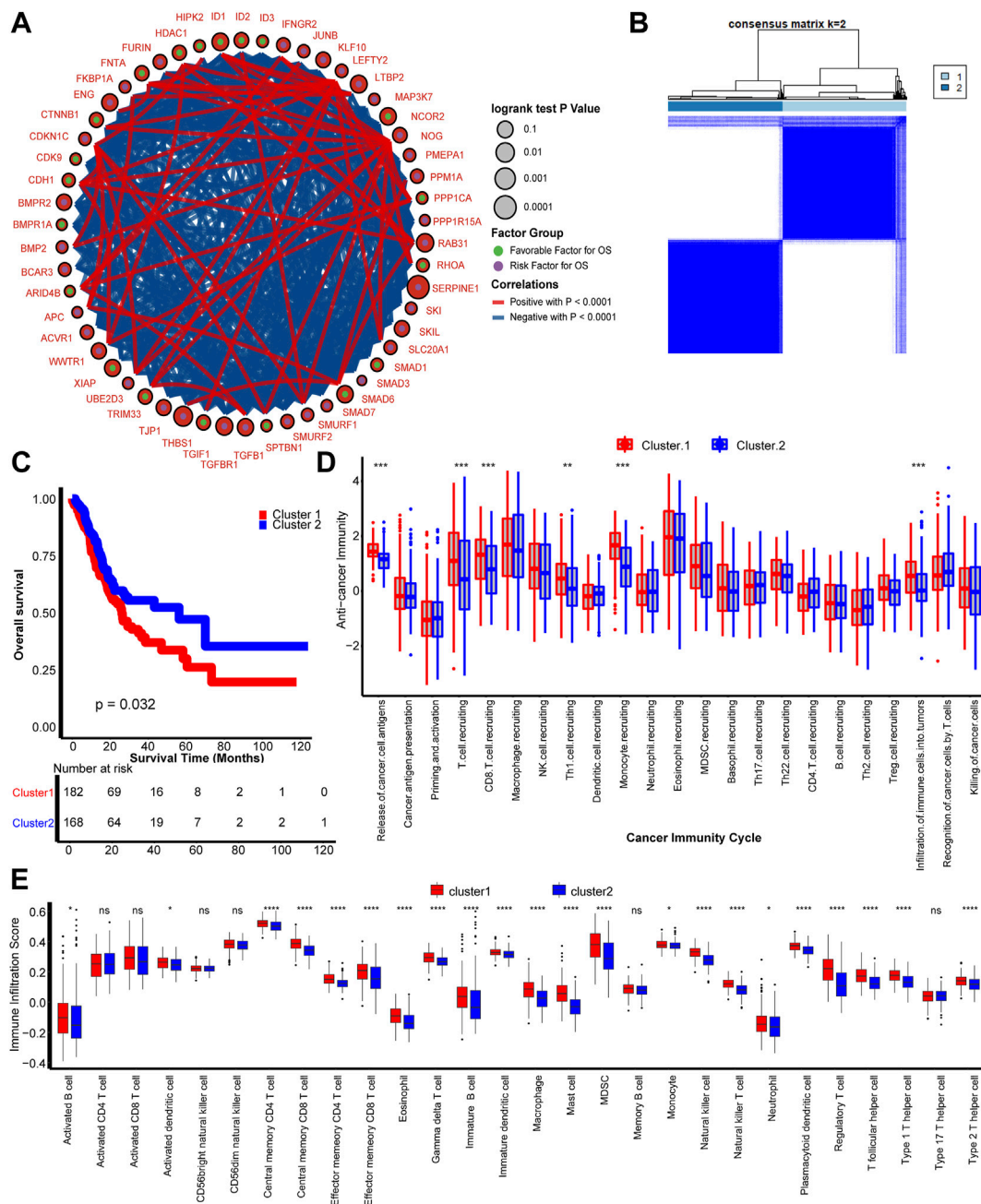


FIGURE 1 | TGF β patterns and corresponding tumor microenvironment infiltration characterization. **(A)** Fifty-four TGF β pathway-related genes correlated with GC. Green and purple dots represent favorable and risk factors for overall survival respectively. The prognosis of each gene is expressed by the size of the circle. Curves between linked dots show the negative (blue) and positive (red) correlation between TGF pathway-related genes. **(B)** The consensus score matrix shows that all samples were grouped into clusters by the value of consensus score groups in different iterations ($k = 2$ in TCGA-STAD). **(C)** Survival analysis based on the TCGA-STAD dataset of TGF β Cluster 1 (red) and TGF β Cluster 2 (blue). **(D)** Different activities of cancer immunity cycles between TGF β Cluster 1 (red) and TGF β Cluster 2 (blue). **(E)** TME immune cell infiltration scores between TGF β Cluster 1 (red) and TGF β Cluster 2 (blue). Ns, not significant; * $p < 0.05$; ** $p < 0.01$; *** $p < 0.001$; **** $p < 0.0001$.

the survival outcomes and TME infiltration of individual patients, we aimed to develop a TGF β -based risk score. WGCNA is a method that can generate modules by similar gene expression patterns and correlate these modules with specific features, generally, clinical information (Langfelder and Horvath, 2008). In this study, we treated TGF β clusters as clinical information and performed

WGCNA combined with other clinical information including, age, sex, grade, T stage, N stage, and M stage to find the module with the closest relationship with TGF β clusters (Figure 2A). Then, we selected 8 as the soft threshold to perform further analysis by setting the scale-free $R^2 = 0.85$ (Figure 2B). Twenty-three modules were filtered according to average hierarchical clustering and dynamic tree

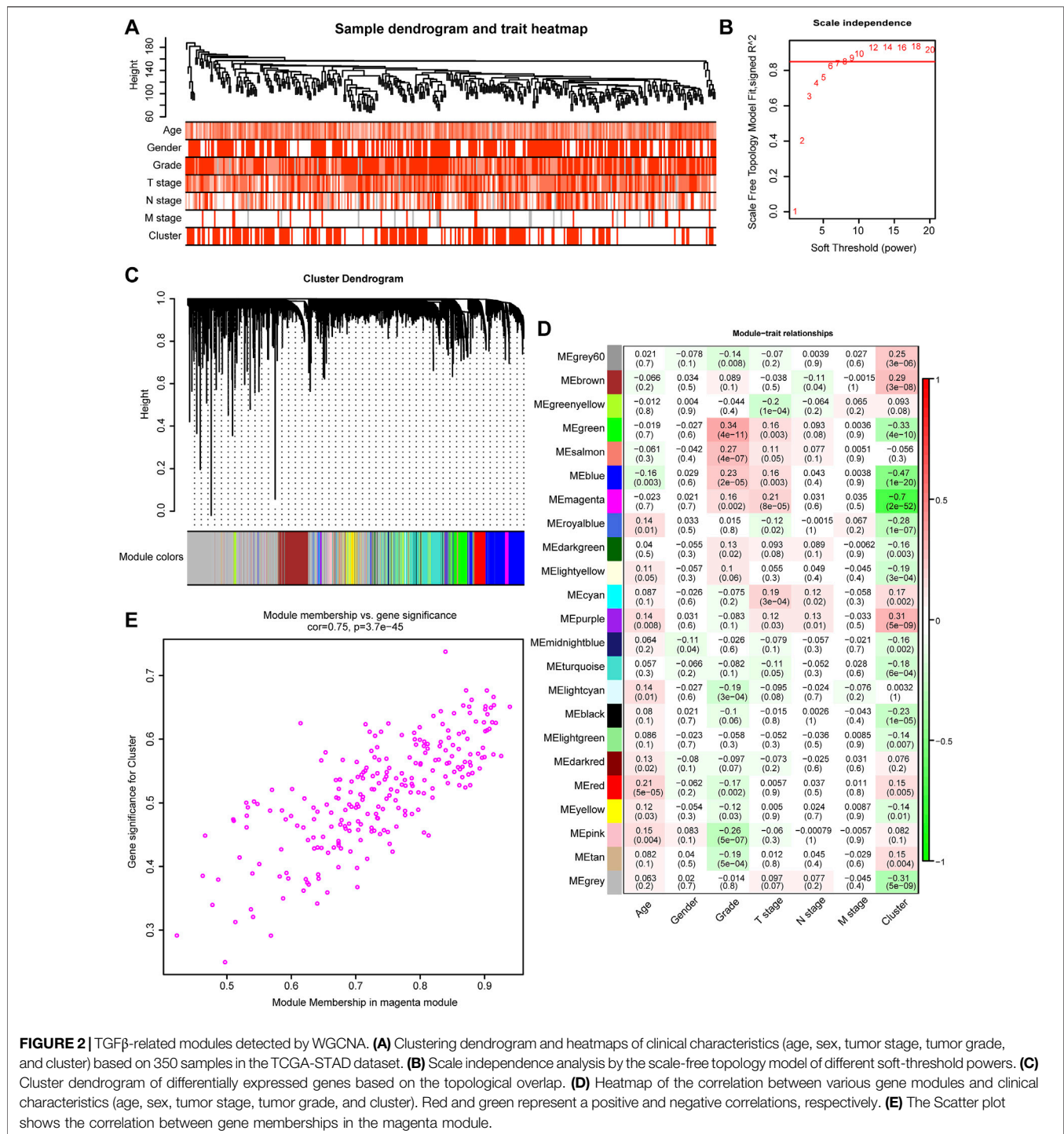


FIGURE 2 | TGF β -related modules detected by WGCNA. **(A)** Clustering dendrogram and heatmaps of clinical characteristics (age, sex, tumor stage, tumor grade, and cluster) based on 350 samples in the TCGA-STAD dataset. **(B)** Scale independence analysis by the scale-free topology model of different soft-threshold powers. **(C)** Cluster dendrogram of differentially expressed genes based on the topological overlap. **(D)** Heatmap of the correlation between various gene modules and clinical characteristics (age, sex, tumor stage, tumor grade, and cluster). Red and green represent a positive and negative correlations, respectively. **(E)** The Scatter plot shows the correlation between gene memberships in the magenta module.

clipping (Figure 2C). The modules with the closest association with clinical information possessed the greatest biological meanings. The magenta module had the closest association with the TGF β clusters ($r = -0.70$, $p < 0.0001$) (Figure 2D). In addition, the magenta module also had a close relationship with tumor grade ($r = 0.16$, $p < 0.002$) and T stage ($r = 0.21$, $p < 0.0001$) (Figure 2D). Further analysis showed that the genes in the magenta module were significantly coexpressed ($cor = 0.75$, $p < 0.0001$, Figure 2E, Supplementary Table S5). KEGG

analysis revealed that genes could be enriched in the TGF β pathway in the magenta module, which confirmed from another perspective that this module had a close relationship with the TGF β pathway (Supplementary Figure S2, Supplementary Table S6). Additionally, extracellular matrix (ECM) organization, extracellular structure organization, collagen-containing extracellular matrix and ECM-receptor interaction pathways were outstanding in GO and KEGG analysis. These results indicated that the genes in the magenta

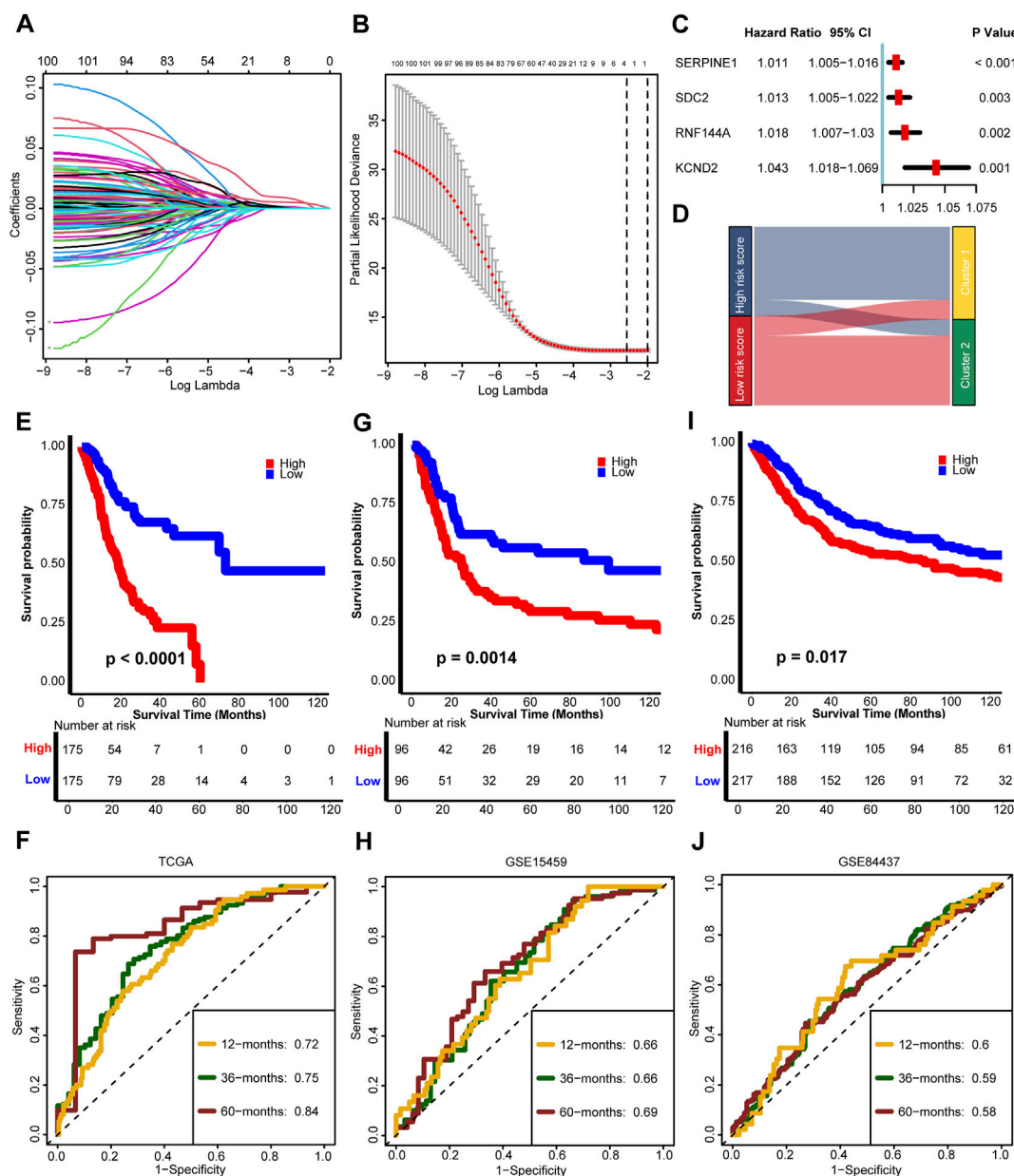


FIGURE 3 | Development and external validation of a TGF β risk score. **(A)** Least absolute shrinkage and selection operator (LASSO) coefficient curves show the log (λ) sequence of 101 prognostic genes in the TCGA-STAD cohort. **(B)** Cross-validation for the selection of turning parameter selection by minimum criteria in the LASSO regression model. Two dotted vertical lines using the minimum criteria were plotted at the optimal values. Four genes with the best discriminative capability were selected to develop the risk score. **(C)** Univariate Cox analysis of 4 predictor genes. **(D)** The relationship between the risk score and TGF β clusters. **(E–J)** Development and validation of the risk score in TCGA-STAD, GSE15459, and GSE84437 databases respectively and the predictive accuracy of the risk score for survival.

module might play a critical role in the TME of GC by regulating the ECM (Supplementary Figure S2, Supplementary Table S7).

Risk Score Development and External Validation

The 243 genes in the magenta module were selected to develop a TGF β associated risk score. First, we filtered 101 genes with

prognostic values by performing univariate Cox regression analysis (Supplementary Table S8) and identified 4 optimal candidates with minimal lambda (0.077) to generate the risk score by using random survival forest analysis (Figures 3A,B). Then we determined the prognostic values of the 4 identified genes (Figure 3C and Supplementary Table S9). By defining the median value of the risk score, we grouped the risk score into high and low risk score groups and found that high risk score group represented TGF β

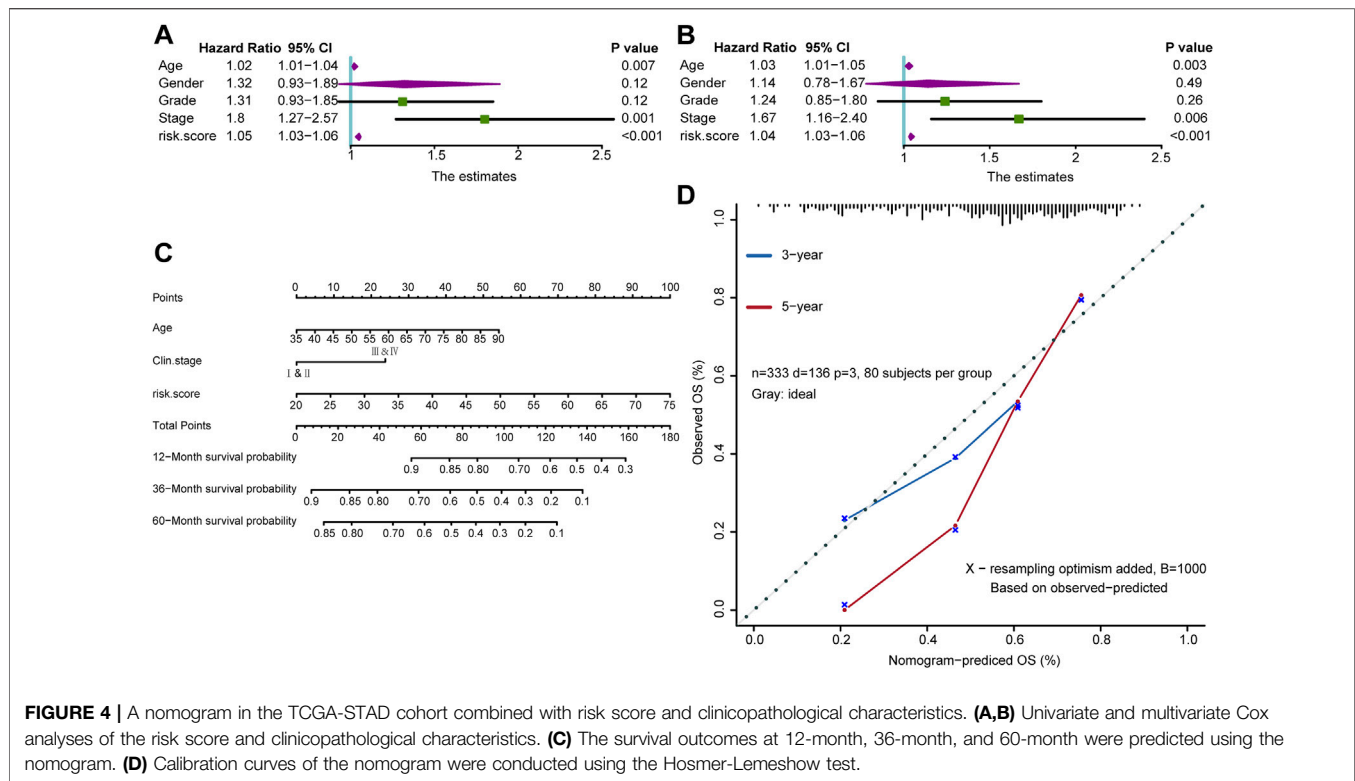


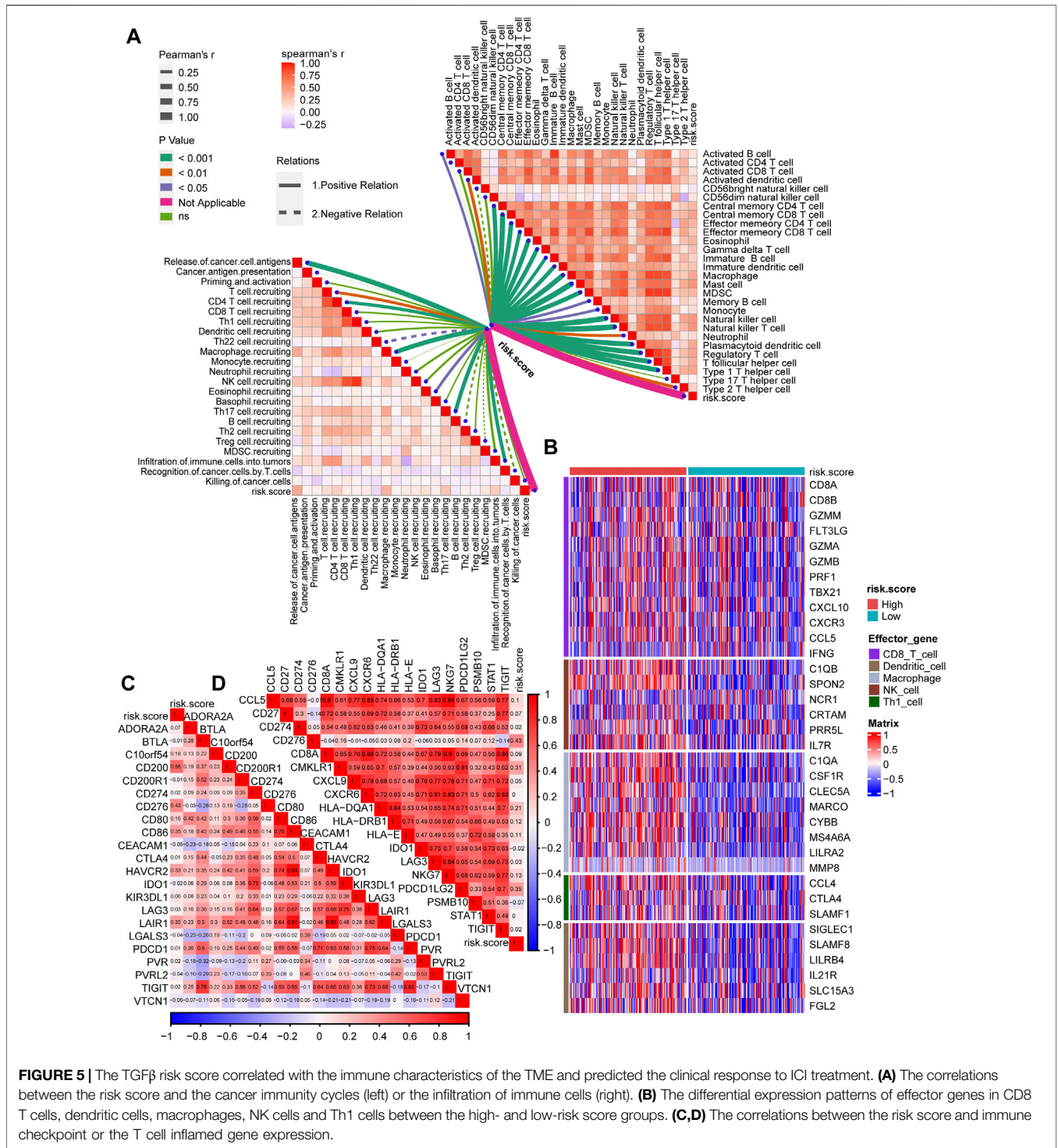
FIGURE 4 | A nomogram in the TCGA-STAD cohort combined with risk score and clinicopathological characteristics. **(A,B)** Univariate and multivariate Cox analyses of the risk score and clinicopathological characteristics. **(C)** The survival outcomes at 12-month, 36-month, and 60-month were predicted using the nomogram. **(D)** Calibration curves of the nomogram were conducted using the Hosmer-Lemeshow test.

Cluster1 while low risk score group represented TGF β Cluster2 (Figure 3D). Consistent with our previous results, the higher risk score group revealed significantly poorer survival outcomes than the lower risk score group ($p < 0.0001$, Figure 3E). The predictive accuracy of the risk score for 12, 36 and 60 months was 0.72, 0.75, and 0.84 respectively (Figure 3F). Notably, we validated this risk score in external databases. Patients in the high-risk score group exhibited significantly poorer survival outcomes ($p = 0.0014$), and the predictive accuracies for 12, 36 and 60 months were 0.66, 0.66, and 0.69, respectively, in the GSE15459 cohort (Figures 3G,H). Meanwhile, in the GSE84437 cohort, a higher risk score was significantly related to poorer survival outcomes ($p = 0.017$), and the predictive accuracies for 12, 36 and 60 months were 0.60, 0.59, and 0.58 respectively (Figures 3I,J).

To investigate the correlation between risk score and clinical information, including age, sex, tumor grade, and TNM stage, we used univariate Cox analysis and the results showed that age, tumor stage, and risk score were all risk factors for GC (Figure 4A, Supplementary Table S10). Further multivariate Cox analysis revealed that age, tumor stage and risk score were still independent prognostic factors (Figure 4B, Supplementary Table S10). These analyses indicated that the risk score might be a potential predictive marker for the prognosis of GC. Moreover, to determine the clinical value of our findings, a nomogram was further developed by integrating the risk score, age, and tumor stage (Figure 4C). Importantly, the calibration curves showed that the predicted OS was highly consistent with the actual OS, which indicates the integrated clinical significance of this nomogram (Figure 4D).

Associations Between Risk Score and Tumor Microenvironment Infiltration

The tumor immune microenvironment state plays a critical role in the fate of cancer cells and immunotherapy efficacy. Thus, the correlations between the risk score and the activities of cancer immunity cycles were analyzed. The release of cancer cell antigens, T cell and macrophage recruitment, infiltration of immune cells and several activities of anticancer immune responses were positively correlated with the risk score (Figure 5A, left; Supplementary Table S11). Furthermore, the infiltration of the 28 immune cells calculated using the ssGSEA algorithm, including activated DCs, central and effector memory CD4 T cells, central and effector memory CD8 T cells, NK cells and Th1 helper cells, was significantly positively correlated with the risk score (Figure 5A, right; Supplementary Table S12). Then, we divided GC patients into the high-risk score and low-risk score groups by setting the median value of the risk score as the cutoff. We determined that the higher risk score group was characterized by higher expression of CD8 T cells, DCs, macrophages, NK cells, and Th1 cells (Figure 5B). Consequently, we proposed that the inflamed phenotype in the high-risk score group may indicate a higher sensitivity to ICI treatment. Furthermore, the risk score was positively related to the expression of a majority of immune checkpoints (such as CD200, CD276, CD86, and LAIR1) (Figure 5C, Supplementary Table S13) and T cell-inflamed gene expression profiles (GEPs) (Figure 5D, Supplementary Table S14), which may indicate better ICI efficacy in GC.



DISCUSSION

As one of the most prominent immunosuppressive cytokines, TGFβ can regulate the generation and functions of numerous immune cells (Li and Flavell, 2008). TGFβ can activate Treg cells and attenuate T cells and DCs directly. Moreover, TGFβ can inhibit NK cells and regulate the behavior of neutrophils and

macrophages. All these effects of TGFβ indicate that it plays a vital role in the formation of an immune suppression TME (Sanjabi et al., 2017). TGFβ contains 32 members of the family, which can be divided into TGFβ subfamilies and bone morphogenetic protein (BMP) subfamilies (David and Massagué, 2018). The roles of TGFβ families in gastrointestinal cancers have been widely reported. Pak et al. (2019) reported that TGFβ1 could

induce the expression of VEGF-C and then promote the lymph-angiogenesis of GC (Pak et al., 2019). Li et al. (2005) reported that TGF β 1 could affect apoptosis and proliferation of GC by regulating p15 and p21 (Li et al., 2005). However, all the studies focused on only one or two members of the TGF β families, but the comprehensive effects of TGF β family have not been reported. In our study, we first divided GC patients into two TGF β regulation patterns using unsupervised clustering analysis and then comprehensively analyzed the relationship between all TGF β families. In addition, we systematically correlated these patterns with the TME of GC and developed a TGF β based risk score to accurately predict the survival outcomes and TME characteristics in GC patients. To the best of our knowledge, our work is the first to provide TGF β -associated prognosis and tumor infiltration characterization in gastric carcinoma.

ICI treatment has shown efficacy in numerous cancer types, including GC (Rosenberg et al., 2016; Nishino et al., 2017; Fuchs et al., 2018). However, only a minority of patients respond to the ICI treatment and the extant biomarkers are not precise enough to be used clinically (Roh et al., 2017; Fuchs et al., 2018; Panda et al., 2018). Exhaustively predictive biomarkers for ICI treatment are urgently needed to maximize the therapeutic benefit and minimize toxic side effects. An increasing number of studies support the concept that the TME plays a vital role in the ICI-based immunotherapy (Lee et al., 2014; Nishino et al., 2017). The TME comprises various cell types (endothelial cells, fibroblasts, immune cells, etc.) and extracellular components (cytokines, growth factors, hormones, extracellular matrix, etc.) that surround tumor cells and are nourished by a vascular network (Wu and Dai, 2017). Tumors characterized by immune activation and T cell infiltration are called hot tumors and have a higher response to immunotherapy (Gajewski, 2015), whereas features of T cell absence or attenuation and lower therapy-response in patients are shown in cold tumors (Liu et al., 2020a). Based on 54 TGF β -pathway-related genes, we identified two different TGF β regulation patterns and found that these two patterns represented inflamed and noninflamed TMEs of GC. ICI treatment might show higher response rates in the inflamed phenotype and these regulation patterns could guide precision immunotherapy treatment in GC. Moreover, we developed a TGF β based risk score to predict an individual's TME characteristics. It has been reported that factors involved in immune checkpoints, including PD-1, PD-L1, LAG-3, and CTLA-4, are more highly expressed in inflamed phenotypes of the TME (Gajewski et al., 2017). A majority of 28 immune checkpoint genes collected from Auslander's study were positively correlated with the risk score (Auslander et al., 2018). Additionally, Mark et al. developed a T cell-inflamed GEP that had robust predictive value for ICI treatment (Ayers et al., 2017). In summary, we found that almost all these genes were positively correlated with the risk score based on TGF β regulation patterns, which could be a robust predictive biomarker for the TME and might have potential value for predicting ICI treatment.

Zhang et al. (2020) assessed patterns of an RNA modification of N6-methyladenosine (m6A) and systematically correlated them with the TME infiltration characterization of GC (Zhang et al., 2020). Similar to their study and our previous study, unsupervised clustering analysis was first used to conduct a comprehensive analysis of multiple genes (Li et al., 2021). These two studies then used multiple genes to perform principal component analysis (PCA) to develop a m6A score for individual patients. In contrast, we then used the LASSO algorithm and cross validation to narrow down variables and filtered only four genes to develop a risk score in this study. Our risk score was much easier to transform to clinical application, as fewer genes needed to be detected. There are numerous gene signatures for risk stratification of GC, such as hypoxia-immune-based microenvironment gene signatures (Liu et al., 2020b), autophagy-related gene signatures (Qiu et al., 2020), metabolism-related gene signatures (Wen et al., 2020), and TP53-associated gene signatures (Nie et al., 2020). However, this is the first study developing a TGF β -associated signature for GC. Moreover, unlike a majority of the studies reported, our study systematically correlated the risk score with TME infiltration characterization. It is worth mentioning that the area under the curve (AUC) for our risk score reached 0.84, which indicated an accurate prediction value of our risk score.

In terms of limitations, we only validated the results in several public cohorts and the relevant mechanisms of TGF β need to be further explored *in vivo* and *in vitro*. In addition, we defined the median of the risk score as the cutoff value in all the validation cohorts, and a better cutoff value needs to be further explored for our risk score. Finally, we did not use prospective clinical trials to validate the clinical value of our risk score.

CONCLUSION

We developed and validated a TGF β -associated signature that could predict the survival outcome and TME immune characteristics of GC. Generally, this signature may aid in precision medicine for GC.

DATA AVAILABILITY STATEMENT

The original contributions presented in the study are included in the article/**Supplementary Material**, further inquiries can be directed to the corresponding author.

AUTHOR CONTRIBUTIONS

SL, ZL and HL performed analyses and drafted the manuscript. HL, XW, ZL and SL searched and downloaded the original datasets from TCGA and GEO. SL, ZL and YW contributed to statistical analyses. SL, YW, and QC edited the pictures. XX conceived and supervised the study. All authors contributed to writing the manuscript. All authors reviewed and approved the final manuscript.

FUNDING

This work was supported by the National Natural Science Foundation of China (81670111) and Hunan Provincial Key Research and Development Program (2019SK2242).

ACKNOWLEDGMENTS

We sincerely thank all participants in the study.

REFERENCES

- Auslander, N., Zhang, G., Lee, J. S., Frederick, D. T., Miao, B., Moll, T., et al. (2018). Robust Prediction of Response to Immune Checkpoint Blockade Therapy in Metastatic Melanoma. *Nat. Med.* 24 (10), 1545–1549. doi:10.1038/s41591-018-0157-9
- Ayers, M., Lunceford, J., Nebozhyn, M., Murphy, E., Loboda, A., Kaufman, D. R., et al. (2017). IFN- γ -related mRNA Profile Predicts Clinical Response to PD-1 Blockade. *J. Clin. Investigation* 127 (8), 2930–2940. doi:10.1172/jci91190
- Battle, E., and Massagué, J. (2019). Transforming Growth Factor- β Signaling in Immunity and Cancer. *Immunity* 50 (4), 924–940. doi:10.1016/j.immuni.2019.03.024
- Charoentong, P., Finotello, F., Angelova, M., Mayer, C., Efremova, M., Rieder, D., et al. (2017). Pan-cancer Immunogenomic Analyses Reveal Genotype-Immunophenotype Relationships and Predictors of Response to Checkpoint Blockade. *Cell Rep.* 18 (1), 248–262. doi:10.1016/j.celrep.2016.12.019
- Chen, D. S., and Mellman, I. (2013). Oncology Meets Immunology: the Cancer-Immunity Cycle. *Immunity* 39 (1), 1–10. doi:10.1016/j.immuni.2013.07.012
- Chen, L., Yuan, L., Wang, Y., Wang, G., Zhu, Y., Cao, R., et al. (2017). Co-expression Network Analysis Identified FCER1G in Association with Progression and Prognosis in Human Clear Cell Renal Cell Carcinoma. *Int. J. Biol. Sci.* 13 (11), 1361–1372. doi:10.7150/ijbs.21657
- Coutzac, C., Pernot, S., Chaput, N., and Zaanan, A. (2019). Immunotherapy in Advanced Gastric Cancer, Is it the Future? *Crit. Rev. oncology/hematology* 133, 25–32. doi:10.1016/j.critrevonc.2018.10.007
- Crispen, P. L., and Kusmartsev, S. (2020). Mechanisms of Immune Evasion in Bladder Cancer. *Cancer Immunol. Immunother.* 69 (1), 3–14. doi:10.1007/s00262-019-02443-4
- David, C. J., and Massagué, J. (2018). Contextual Determinants of TGF β Action in Development, Immunity and Cancer. *Nat. Rev. Mol. Cell Biol.* 19 (7), 419–435. doi:10.1038/s41580-018-0007-0
- Fuchs, C. S., Doi, T., Jang, R. W., Muro, K., Satoh, T., Machado, M., et al. (2018). Safety and Efficacy of Pembrolizumab Monotherapy in Patients with Previously Treated Advanced Gastric and Gastroesophageal Junction Cancer. *JAMA Oncol.* 4 (5), e180013. doi:10.1001/jamaoncol.2018.0013
- Gajewski, T. F., Corrales, L., Williams, J., Horton, B., Sivan, A., and Spranger, S. (2017). Cancer Immunotherapy Targets Based on Understanding the T Cell-Inflamed versus Non-T Cell-Inflamed Tumor Microenvironment. *Adv. Exp. Med. Biol.* 1036, 19–31. doi:10.1007/978-3-319-67577-0_2
- Gajewski, T. F. (2015). The Next Hurdle in Cancer Immunotherapy: Overcoming the Non-T-cell-inflamed Tumor Microenvironment. *Seminars Oncol.* 42 (4), 663–671. doi:10.1053/j.seminoncol.2015.05.011
- Goldman, M. J., Craft, B., Hastie, M., Repčička, K., McDade, F., Kamath, A., et al. (2020). Visualizing and Interpreting Cancer Genomics Data via the Xena Platform. *Nat. Biotechnol.* 38 (6), 675–678. doi:10.1038/s41587-020-0546-8
- Hu, J., Yu, A., Othmane, B., Qiu, D., Li, H., Li, C., et al. (2021). Siglec15 Shapes a Non-inflamed Tumor Microenvironment and Predicts the Molecular Subtype in Bladder Cancer. *Theranostics* 11 (7), 3089–3108. doi:10.7150/thno.53649
- Hugo, W., Zaretsky, J. M., Sun, L., Song, C., Moreno, B. H., Hu-Lieskovan, S., et al. (2016). Genomic and Transcriptomic Features of Response to Anti-PD-1 Therapy in Metastatic Melanoma. *Cell* 165 (1), 35–44. doi:10.1016/j.cell.2016.02.065

SUPPLEMENTARY MATERIAL

The Supplementary Material for this article can be found online at: <https://www.frontiersin.org/articles/10.3389/fgene.2022.818378/full#supplementary-material>

Supplementary Figure S1 | (A–E) The consensus score matrix when $k = 3, 4$ and 5 for all samples in TCGA-STAD. **(F)** GSEA analysis shows the enrichment of angiogenesis related pathways between TGF β clusters.

Supplementary Figure S2 | GO and KEGG analysis of the TGF β -pathway-related genes in the magenta module.

- Janjigian, Y. Y., Bendell, J., Calvo, E., Kim, J. W., Ascierto, P. A., Sharma, P., et al. (2018). CheckMate-032 Study: Efficacy and Safety of Nivolumab and Nivolumab Plus Ipilimumab in Patients with Metastatic Esophagogastric Cancer. *Jco* 36 (28), 2836–2844. doi:10.1200/jco.2017.76.6212
- Kang, Y.-K., Boku, N., Satoh, T., Ryu, M.-H., Chao, Y., Kato, K., et al. (2017). Nivolumab in Patients with Advanced Gastric or Gastro-Oesophageal Junction Cancer Refractory to, or Intolerant of, at Least Two Previous Chemotherapy Regimens (ONO-4538-12, ATTRACTION-2): a Randomised, Double-Blind, Placebo-Controlled, Phase 3 Trial. *Lancet* 390 (10111), 2461–2471. doi:10.1016/s0140-6736(17)31827-5
- Langfelder, P., and Horvath, S. (2008). WGCNA: an R Package for Weighted Correlation Network Analysis. *BMC Bioinforma.* 9, 559. doi:10.1186/1471-2105-9-559
- Lee, K., Hwang, H., and Nam, K. T. (2014). Immune Response and the Tumor Microenvironment: How They Communicate to Regulate Gastric Cancer. *Gut Liver* 8 (2), 131–139. doi:10.5009/gnl.2014.8.2.131
- Li, H., Hu, J., Yu, A., Othmane, B., Guo, T., Liu, J., et al. (2021). RNA Modification of N6-Methyladenosine Predicts Immune Phenotypes and Therapeutic Opportunities in Kidney Renal Clear Cell Carcinoma. *Front. Oncol.* 11, 642159. doi:10.3389/fgene.2021.642159
- Li, M. O., and Flavell, R. A. (2008). Contextual Regulation of Inflammation: A Duet by Transforming Growth Factor- β and Interleukin-10. *Immunity* 28 (4), 468–476. doi:10.1016/j.immuni.2008.03.003
- Li, X., Zhang, Y. Y., Wang, Q., and Fu, S. B. (2005). Association between Endogenous Gene Expression and Growth Regulation Induced by TGF-B1 in Human Gastric Cancer Cells. *Wjg* 11 (1), 61–68. doi:10.3748/wjg.v11.i1.61
- Liu, Y., Wu, J., Huang, W., Weng, S., Wang, B., Chen, Y., et al. (2020). Development and Validation of a Hypoxia-Immune-Based Microenvironment Gene Signature for Risk Stratification in Gastric Cancer. *J. Transl. Med.* 18 (1), 201. doi:10.1186/s12967-020-02366-0
- Liu, Z., Han, C., and Fu, Y.-X. (2020). Targeting Innate Sensing in the Tumor Microenvironment to Improve Immunotherapy. *Cell Mol. Immunol.* 17 (1), 13–26. doi:10.1038/s41423-019-0341-y
- Mariathasan, S., Turley, S. J., Nickles, D., Castiglioni, A., Yuen, K., Wang, Y., et al. (2018). TGF β Attenuates Tumour Response to PD-L1 Blockade by Contributing to Exclusion of T Cells. *Nature* 554 (7693), 544–548. doi:10.1038/nature25501
- Nie, K., Zheng, Z., Wen, Y., Shi, L., Xu, S., Wang, X., et al. (2020). Construction and Validation of a TP53-Associated Immune Prognostic Model for Gastric Cancer. *Genomics* 112 (6), 4788–4795. doi:10.1016/j.ygeno.2020.08.026
- Nishino, M., Ramaiya, N. H., Hatabu, H., and Hodi, F. S. (2017). Monitoring Immune-Checkpoint Blockade: Response Evaluation and Biomarker Development. *Nat. Rev. Clin. Oncol.* 14 (11), 655–668. doi:10.1038/nrclinonc.2017.88
- Pak, K. H., Park, K. C., and Cheong, J.-H. (2019). VEGF-C Induced by TGF- β 1 Signaling in Gastric Cancer Enhances Tumor-Induced Lymphangiogenesis. *BMC cancer* 19 (1), 799. doi:10.1186/s12885-019-5972-y
- Panda, A., Mehnert, J. M., Hirshfield, K. M., Riedlinger, G., Damare, S., Saunders, T., et al. (2018). Immune Activation and Benefit from Avelumab in EBV-Positive Gastric Cancer. *J. Natl. Cancer Inst.* 110 (3), 316–320. doi:10.1093/jnci/djx213
- Qiu, J., Sun, M., Wang, Y., and Chen, B. (2020). Identification and Validation of an Individualized Autophagy-Clinical Prognostic Index in Gastric Cancer Patients. *Cancer Cell Int.* 20, 178. doi:10.1186/s12935-020-01267-y

- Roh, W., Chen, P.-L., Reuben, A., Spencer, C. N., Prieto, P. A., Miller, J. P., et al. (2017). Integrated Molecular Analysis of Tumor Biopsies on Sequential CTLA-4 and PD-1 Blockade Reveals Markers of Response and Resistance. *Sci. Transl. Med.* 9 (379). doi:10.1126/scitranslmed.aah3560
- Rosenberg, J. E., Hoffman-Censits, J., Powles, T., van der Heijden, M. S., Balar, A. V., Necchi, A., et al. (2016). Atezolizumab in Patients with Locally Advanced and Metastatic Urothelial Carcinoma Who Have Progressed Following Treatment with Platinum-Based Chemotherapy: a Single-Arm, Multicentre, Phase 2 Trial. *Lancet* 387 (10031), 1909–1920. doi:10.1016/s0140-6736(16)00561-4
- Sanjabi, S., Oh, S. A., and Li, M. O. (2017). Regulation of the Immune Response by TGF- β : From Conception to Autoimmunity and Infection. *Cold Spring Harb. Perspect. Biol.* 9 (6), a022236. doi:10.1101/cshperspect.a022236
- Smyth, E. C., Nilsson, M., Grabsch, H. I., van Grieken, N. C., and Lordick, F. (2020). Gastric Cancer. *Lancet* 396 (10251), 635–648. doi:10.1016/s0140-6736(20)31288-5
- Veen, L. M., Skrabanja, T. L. P., Derks, S., de Gruijl, T. D., Bijlsma, M. F., and van Laarhoven, H. W. M. (2021). The Role of Transforming Growth Factor β in Upper Gastrointestinal Cancers: A Systematic Review. *Cancer Treat. Rev.* 100, 102285. doi:10.1016/j.ctrv.2021.102285
- Vrána, D., Matzenauer, M., Neoral, Č., Auješký, R., Vrba, R., Melichar, B., et al. (2018). From Tumor Immunology to Immunotherapy in Gastric and Esophageal Cancer. *Ijms* 20 (1), 13. doi:10.3390/ijms20010013
- Wen, F., Huang, J., Lu, X., Huang, W., Wang, Y., Bai, Y., et al. (2020). Identification and Prognostic Value of Metabolism-Related Genes in Gastric Cancer. *Aging* 12 (17), 17647–17661. doi:10.18632/aging.103838
- Wilkerson, M. D., and Hayes, D. N. (2010). ConsensusClusterPlus: a Class Discovery Tool with Confidence Assessments and Item Tracking. *Bioinforma. Oxf. Engl.* 26 (12), 1572–1573. doi:10.1093/bioinformatics/btq1170
- Wu, T., and Dai, Y. (2017). Tumor Microenvironment and Therapeutic Response. *Cancer Lett.* 387, 61–68. doi:10.1016/j.canlet.2016.01.043
- Xu, L., Deng, C., Pang, B., Zhang, X., Liu, W., Liao, G., et al. (2018). TIP: A Web Server for Resolving Tumor Immunophenotype Profiling. *Cancer Res.* 78 (23), 6575–6580. doi:10.1158/0008-5472.Can-18-0689
- Zhang, B., Wu, Q., Li, B., Wang, D., Wang, L., and Zhou, Y. L. (2020). m6A Regulator-Mediated Methylation Modification Patterns and Tumor Microenvironment Infiltration Characterization in Gastric cancerA Regulator-Mediated Methylation Modification Patterns and Tumor Microenvironment Infiltration Characterization in Gastric Cancer. *Mol. Cancer* 19 (1), 53. doi:10.1186/s12943-020-01170-0

Conflict of Interest: The authors declare that the research was conducted in the absence of any commercial or financial relationships that could be construed as a potential conflict of interest.

Publisher's Note: All claims expressed in this article are solely those of the authors and do not necessarily represent those of their affiliated organizations, or those of the publisher, the editors and the reviewers. Any product that may be evaluated in this article, or claim that may be made by its manufacturer, is not guaranteed or endorsed by the publisher.

Copyright © 2022 Liu, Li, Li, Wen, Wang, Chen and Xu. This is an open-access article distributed under the terms of the Creative Commons Attribution License (CC BY). The use, distribution or reproduction in other forums is permitted, provided the original author(s) and the copyright owner(s) are credited and that the original publication in this journal is cited, in accordance with accepted academic practice. No use, distribution or reproduction is permitted which does not comply with these terms.